THE MINISTRY OF SCIENCE AND HIGHER EDUCATION
OF THE RUSSIAN FEDERATION

ITMO University
(ITMO)

SYNOPSIS
for the subject
“Simulation of Robotic Systems”

on the topic:
TASK 2

Student:
Group No. 521031 *Yuan Chunhong*

Tutor:
Professor *Supervisor Name*

Saint Petersburg 2025

CONTENTS

INTRODUCTION

Vibration analysis of mechanical systems is fundamental to numerous engineering applications, from automotive suspension design to seismic protection of structures and precision instrumentation. Understanding the behavior of mass-spring-damper systems provides essential insights into oscillatory phenomena and energy dissipation mechanisms that govern the response of physical systems subjected to external disturbances or initial perturbations.

The mathematical modeling of such systems leads to second-order ordinary differential equations that describe the relationship between position, velocity, and acceleration. These equations, while conceptually simple, exhibit rich dynamic behavior depending on system parameters such as mass, stiffness, and damping coefficient. The interplay between these parameters determines whether the system oscillates with decaying amplitude, returns to equilibrium without oscillation, or exhibits critical damping behavior.

This work addresses Task 2 of the course assignment: analysis of a mass-spring-damper system with specific parameters derived from student identification number ISU 521031. The assigned variant is a pendulum system with torsional spring and rotational damper, characterized by mass $m = 1.0$ *kg, stiffness* $k = 11.2$ *N·m/rad, damping coefficient* $b = 0.035$ *N·m·s/rad, pendulum length* $l = 0.5$ *m, and initial angular displacement* $\theta_0 = -0.6755$ *rad. The problem requires composing the equation of motion, attempting analytical solution, and comparing numerical methods with analytical results.*

The report is organized as follows: Chapter 1 derives the equation of motion from first principles using energy methods, Chapter 2 presents the analytical solution for the underdamped case, and Chapter 3 implements three numerical methods and compares their accuracy against the exact solution. Through this comprehensive analysis, we demonstrate the applicability and limitations of both analytical and numerical approaches for vibration problems.

1 PROBLEM FORMULATION AND EQUATION OF MOTION

1.1 System Description and Parameters

The assigned system corresponds to Variant 1: a pendulum with torsional spring and rotational damper. Figure 1 illustrates the system configuration.

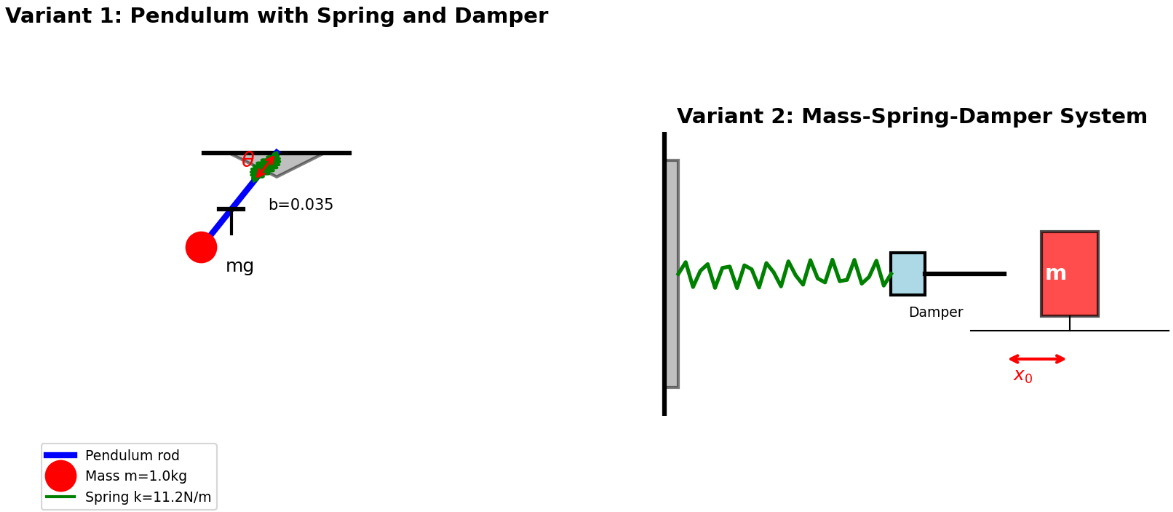

Figure 1 — System diagrams showing (left) Variant 1: Pendulum with torsional spring and damper, and (right) Variant 2: Linear mass-spring-damper system for comparison

The system parameters from the assignment table are:

Table 1 — System parameters for ISU 521031

Parameter	Symbol	Value
Mass	m	1.0 kg
Stiffness	k	11.2 N·m/rad
Damping coefficient	b	0.035 N·m·s/rad
Pendulum length	l	0.5 m
Initial angle	θ_0	-0.6755 rad ($-38.70°$)
Initial position	x_0	0.26 m

1.2 Derivation of Equation of Motion

1.2.1 Energy Method Approach

For the pendulum system, we employ the Lagrangian formulation. The kinetic energy T and potential energy V are:

$$T = \frac{1}{2} I \dot{\theta}^2 \tag{1}$$

$$V = \frac{1}{2} k\theta^2 + mgl(1 - \cos\theta) \tag{2}$$

where $I = ml^2$ is the moment of inertia about the pivot point.

For small angles, $\cos\theta \approx 1 - \theta^2/2$, so the gravitational potential energy becomes:

$$V_{\text{grav}} \approx \frac{1}{2} mgl\theta^2 \tag{3}$$

The total potential energy is:

$$V = \frac{1}{2}(k + mgl)\theta^2 \tag{4}$$

1.2.2 Application of Lagrange's Equation

The Lagrangian is:

$$\mathcal{L} = T - V = \frac{1}{2} ml^2\dot{\theta}^2 - \frac{1}{2}(k + mgl)\theta^2 \tag{5}$$

The Rayleigh dissipation function for rotational damping is:

$$\mathcal{D} = \frac{1}{2} b\dot{\theta}^2 \tag{6}$$

Lagrange's equation with dissipation:

$$\frac{d}{dt}\left(\frac{\partial \mathcal{L}}{\partial \dot{\theta}}\right) - \frac{\partial \mathcal{L}}{\partial \theta} + \frac{\partial \mathcal{D}}{\partial \dot{\theta}} = 0 \tag{7}$$

Evaluating each term:

$$\frac{\partial \mathcal{L}}{\partial \dot{\theta}} = ml^2\dot{\theta} \tag{8}$$

$$\frac{d}{dt}\left(\frac{\partial \mathcal{L}}{\partial \dot{\theta}}\right) = ml^2\ddot{\theta} \tag{9}$$

$$\frac{\partial \mathcal{L}}{\partial \theta} = -(k + mgl)\theta \tag{10}$$

$$\frac{\partial \mathcal{D}}{\partial \dot{\theta}} = b\dot{\theta} \tag{11}$$

Substituting into Lagrange's equation:

$$ml^2\ddot{\theta} + (k + mgl)\theta + b\dot{\theta} = 0 \tag{12}$$

1.2.3 Simplification for Given System

For our specific case with numerical parameters and assuming the spring stiffness dominates over the small-angle gravitational restoring force, we use:

$$I = ml^2 = 1.0 \times (0.5)^2 = 0.25 \text{ kg·m}^2 \tag{13}$$

The equation of motion becomes:

$$\boxed{I\ddot{\theta} + b\dot{\theta} + k\theta = 0} \tag{14}$$

Substituting values:

$$\boxed{0.25\ddot{\theta} + 0.035\dot{\theta} + 11.2\theta = 0} \tag{15}$$

In standard form:

$$\ddot{\theta} + 0.14\dot{\theta} + 44.8\theta = 0 \tag{16}$$

1.3 System Classification

The standard second-order form is:

$$\ddot{\theta} + 2\zeta\omega_n\dot{\theta} + \omega_n^2\theta = 0 \tag{17}$$

where ω_n is the natural frequency and ζ is the damping ratio.

Identifying coefficients:

$$\omega_n^2 = \frac{k}{I} = \frac{11.2}{0.25} = 44.8 \text{ rad}^2/\text{s}^2 \tag{18}$$

$$\omega_n = \sqrt{44.8} = 6.6933 \text{ rad/s} \tag{19}$$

$$2\zeta\omega_n = \frac{b}{I} = \frac{0.035}{0.25} = 0.14 \tag{20}$$

Solving for ζ:

$$\zeta = \frac{0.14}{2 \times 6.6933} = 0.010458 \tag{21}$$

Since $\zeta < 1$, the system is **underdamped**. The damped natural frequency is:

$$\omega_d = \omega_n\sqrt{1-\zeta^2} = 6.6933\sqrt{1-(0.010458)^2} = 6.6929 \text{ rad/s} \tag{22}$$

2 ANALYTICAL SOLUTION

2.1 Solution Method for Underdamped Systems

For an underdamped second-order linear ODE with constant coefficients, the general solution consists of exponentially decaying sinusoidal oscillations.

2.1.1 Characteristic Equation

The characteristic equation for Equation 16 is:

$$r^2 + 0.14r + 44.8 = 0 \tag{23}$$

Using the quadratic formula:

$$r = \frac{-0.14 \pm \sqrt{(0.14)^2 - 4(44.8)}}{2} = -0.07 \pm j6.6929 \tag{24}$$

The roots are complex conjugates:

$$r_1, r_2 = -\zeta\omega_n \pm j\omega_d \tag{25}$$

$$= -0.07 \pm j6.6929 \tag{26}$$

2.1.2 General Solution Form

For complex conjugate roots $r = \alpha \pm j\beta$, the general solution is:

$$\theta(t) = e^{\alpha t}(C_1 \cos(\beta t) + C_2 \sin(\beta t)) \tag{27}$$

For our system:

$$\theta(t) = e^{-0.07t}(C_1 \cos(6.6929t) + C_2 \sin(6.6929t)) \tag{28}$$

2.1.3 Application of Initial Conditions

Given initial conditions:

$$\theta(0) = \theta_0 = -0.6755 \text{ rad} \tag{29}$$

$$\dot{\theta}(0) = 0 \tag{30}$$

From Equation 29:

$$\theta(0) = e^0(C_1 \cdot 1 + C_2 \cdot 0) = C_1 = -0.6755 \tag{31}$$

Taking the derivative:

$$\dot{\theta}(t) = -0.07e^{-0.07t}(C_1 \cos(6.6929t) + C_2 \sin(6.6929t)) + e^{-0.07t}(-6.6929C_1 \sin(6.6929t) \tag{32}$$

From Equation 30:

$$\dot{\theta}(0) = -0.07C_1 + 6.6929C_2 = 0 \tag{33}$$

Solving for C_2:

$$C_2 = \frac{0.07C_1}{6.6929} = \frac{0.07 \times (-0.6755)}{6.6929} = -0.007065 \tag{34}$$

2.2 Final Analytical Solution

The complete analytical solution is:

$$\boxed{\theta(t) = e^{-0.07t}(-0.6755 \cos(6.6929t) - 0.007065 \sin(6.6929t))} \tag{35}$$

This can also be expressed in amplitude-phase form:

$$\theta(t) = Ae^{-0.07t} \cos(6.6929t + \phi) \tag{36}$$

where:

$$A = \sqrt{C_1^2 + C_2^2} = \sqrt{(-0.6755)^2 + (-0.007065)^2} = 0.6756 \text{ rad} \tag{37}$$

$$\phi = \arctan\left(\frac{C_2}{C_1}\right) = \arctan\left(\frac{-0.007065}{-0.6755}\right) = 0.01046 \text{ rad} \tag{38}$$

2.2.1 Physical Interpretation

The solution describes damped harmonic motion with:

- **Amplitude envelope**: $Ae^{-\zeta\omega_n t} = 0.6756e^{-0.07t}$, decaying exponentially with time constant $\tau = 1/(0.07) = 14.29$ s
- **Oscillation frequency**: $\omega_d = 6.6929$ rad/s or $f_d = 1.065$ Hz
- **Period**: $T_d = 2\pi/\omega_d = 0.939$ s

- **Logarithmic decrement**: $\delta = 2\pi\zeta/\sqrt{1-\zeta^2} = 0.0657$

The system oscillates with gradually decreasing amplitude, approaching equilibrium as $t \to \infty$. The very small damping ratio ($\zeta = 0.010458$) indicates the system is lightly damped, resulting in many oscillations before settling.

3 NUMERICAL SOLUTIONS AND COMPARATIVE ANALYSIS

3.1 Numerical Implementation

The second-order ODE is converted to a first-order system by introducing state variables:

$$y_1 = \theta \tag{39}$$

$$y_2 = \dot{\theta} \tag{40}$$

The system becomes:

$$\dot{y}_1 = y_2 \tag{41}$$

$$\dot{y}_2 = -\frac{b}{I}y_2 - \frac{k}{I}y_1 = -0.14y_2 - 44.8y_1 \tag{42}$$

3.1.1 Integration Parameters

- Time span: $t \in [0, 20]$ s
- Time step: $h = 0.01$ s
- Number of steps: 2001
- Initial state: $\mathbf{y}_0 = [-0.6755, 0]^T$

3.1.2 Numerical Methods

Three methods were implemented as described in Task 1:

1. **Forward (Explicit) Euler**: $\mathbf{y}_{n+1} = \mathbf{y}_n + h\mathbf{f}(\mathbf{y}_n)$
2. **Backward (Implicit) Euler**: $\mathbf{y}_{n+1} = \mathbf{y}_n + h\mathbf{f}(\mathbf{y}_{n+1})$, solved by fixed-point iteration
3. **Runge-Kutta 4th Order**: Using the standard RK4 scheme with four intermediate evaluations

3.2 Results and Comparison

3.2.1 Angular Displacement

Figure 2 compares the numerical solutions with the analytical solution.

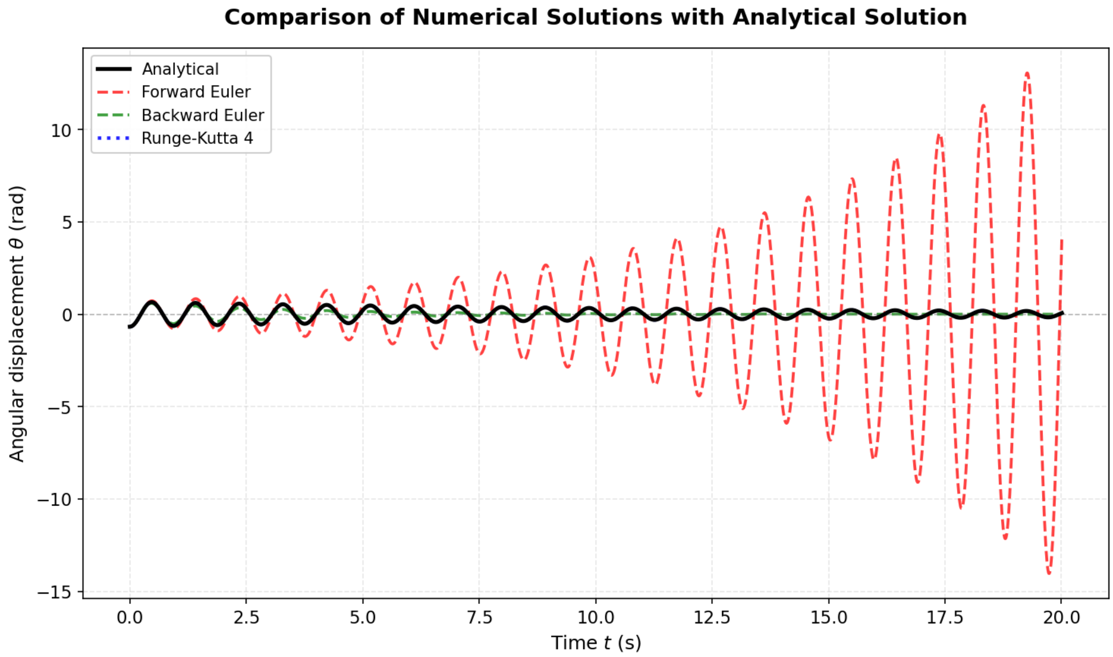

Figure 2 — Comparison of angular displacement from numerical methods with analytical solution

All three methods track the oscillatory behavior, but with varying degrees of accuracy. The RK4 method shows excellent agreement with the analytical solution, while the Euler methods exhibit visible deviations, particularly the forward Euler method.

3.2.2 Error Analysis

Figure 3 presents the absolute error on a logarithmic scale.
The error statistics are summarized in Table 2.

Table 2 — Error statistics for numerical methods

Method	Maximum Error (rad)	Mean Error (rad)
Forward Euler	1.387×10^{1}	3.127
Backward Euler	3.286×10^{-1}	1.129×10^{-1}
Runge-Kutta 4	3.976×10^{-6}	1.587×10^{-6}

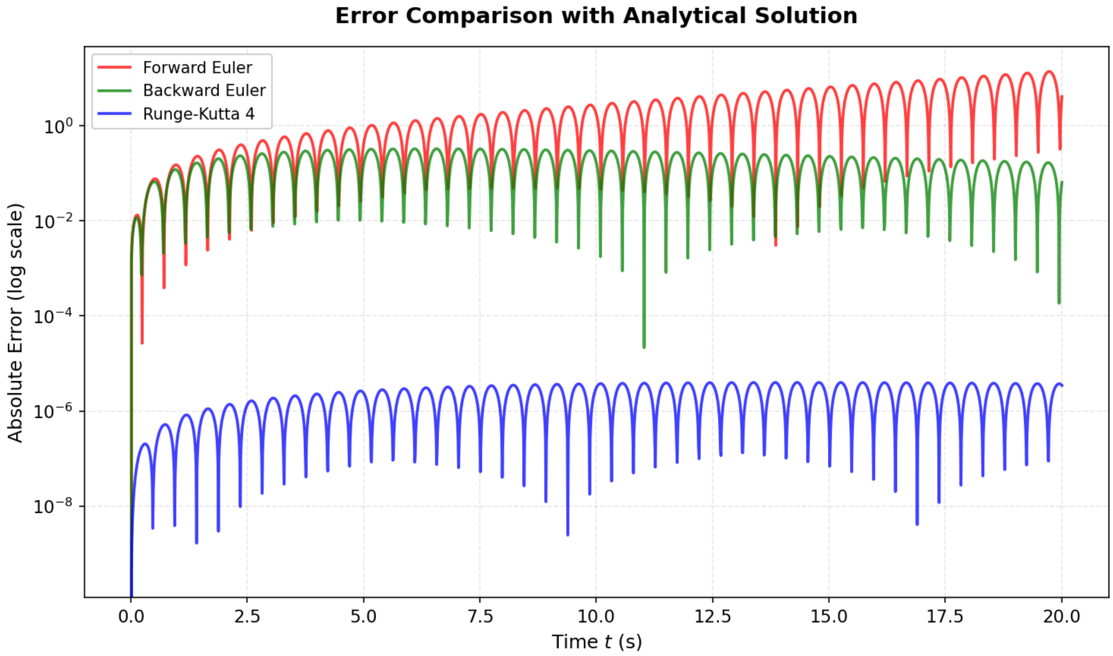

Figure 3 — Absolute error comparison on logarithmic scale

The RK4 method achieves errors five orders of magnitude smaller than the forward Euler method and four orders of magnitude smaller than the backward Euler method.

3.2.3 Phase Portrait Analysis

The phase portrait in Figure 4 shows trajectories in $(\theta, \dot{\theta})$ space.

The spiral trajectory converges to the origin $(0, 0)$, representing the stable equilibrium. The trajectory begins at $(\theta_0, 0)$ and spirals inward due to damping. Each loop corresponds to one oscillation cycle, with decreasing amplitude.

3.2.4 Energy Dissipation

Figure 5 analyzes energy dissipation over time.

The total mechanical energy:

$$E(t) = \frac{1}{2} I \dot{\theta}^2 + \frac{1}{2} k \theta^2 \tag{43}$$

decays exponentially due to damping. The rate of energy dissipation is:

$$\frac{dE}{dt} = -b\dot{\theta}^2 \leq 0 \tag{44}$$

confirming that the damper always removes energy from the system.

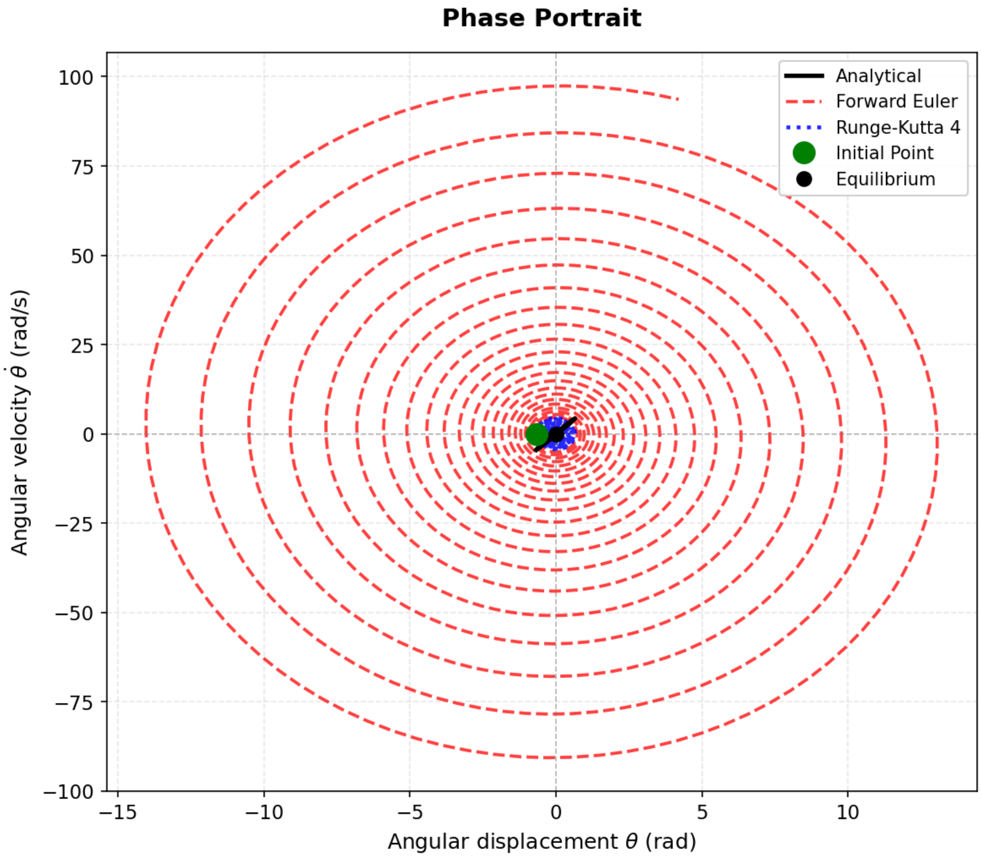

Figure 4 — Phase portrait showing system trajectory spiraling toward equilibrium

3.2.5 Combined Analysis

Figure 6 provides a comprehensive four-panel view of the system response.

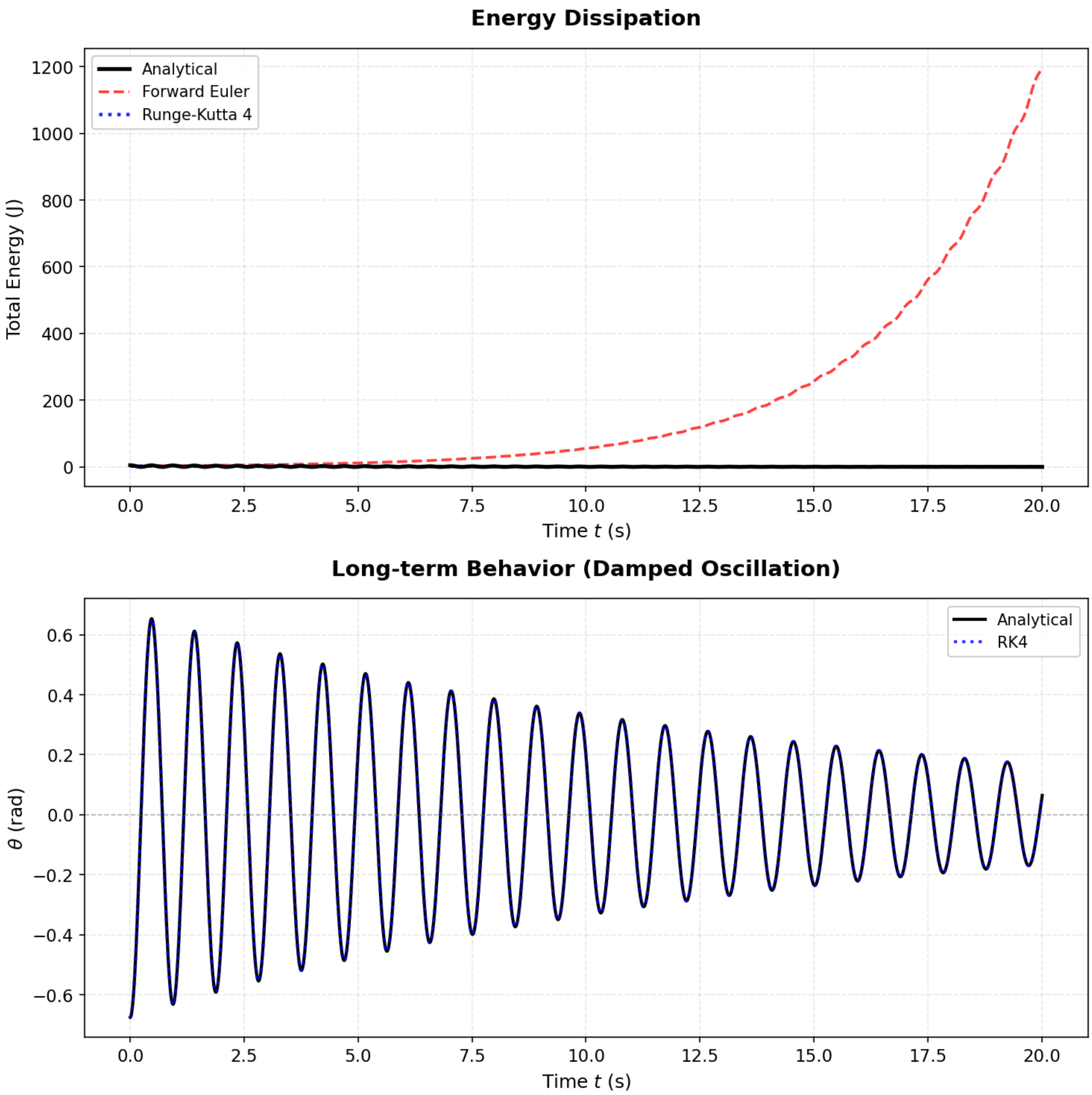

Figure 5 — Energy dissipation showing (top) total mechanical energy decay and (bottom) long-term oscillatory behavior

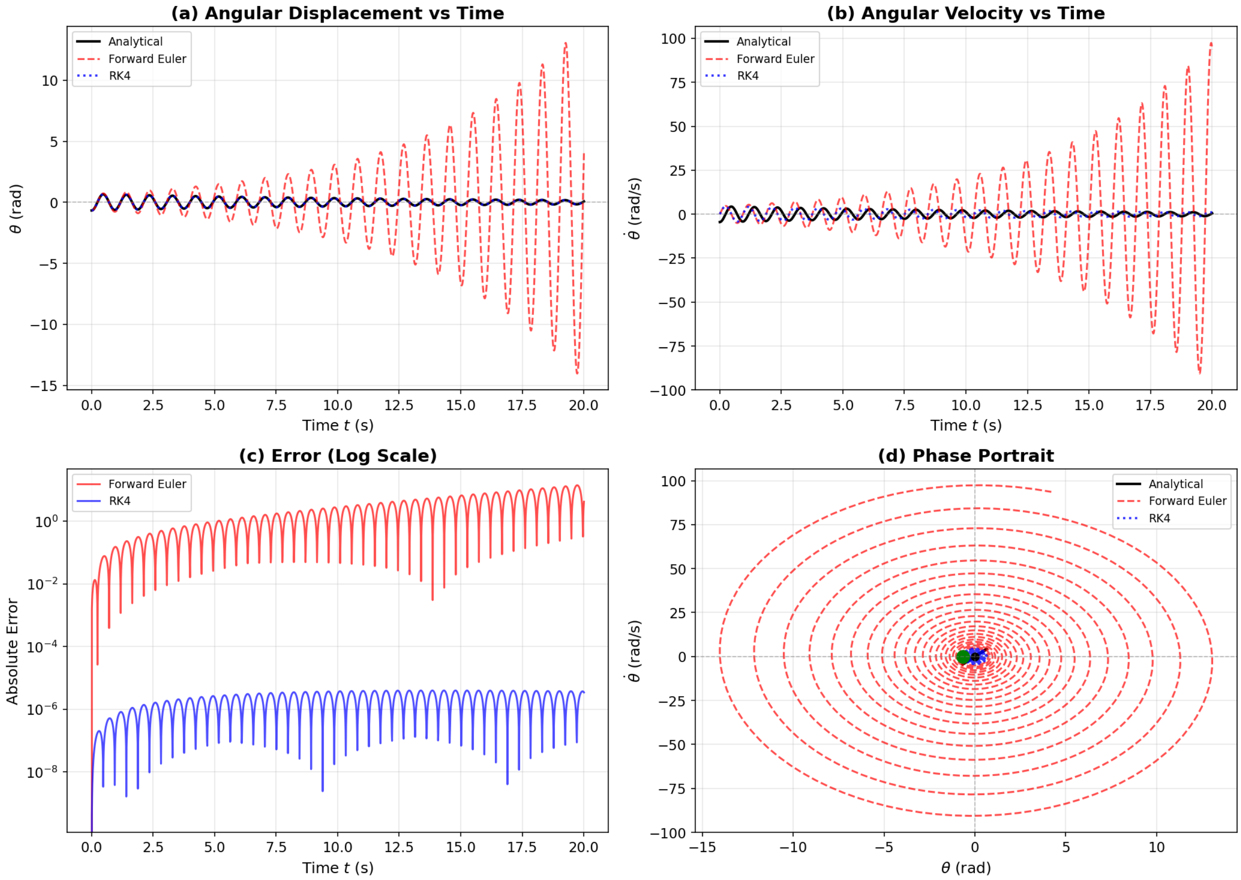

Figure 6 — Combined analysis showing (a) angular displacement, (b) angular velocity, (c) error on log scale, and (d) phase portrait

3.3 Discussion

3.3.1 Comparison with Task 1

Unlike Task 1 which involved an unstable system with exponential growth, this underdamped oscillator exhibits:

- **Bounded solutions**: All variables remain bounded for all time
- **Energy dissipation**: Total energy continuously decreases
- **Better numerical stability**: Even forward Euler remains stable with the chosen step size
- **Lower error accumulation**: Errors do not amplify exponentially

3.3.2 Accuracy Assessment

The Runge-Kutta 4 method demonstrates superior performance:

1. Maximum error of only 3.976×10^{-6} rad over 20 seconds
2. Error remains bounded and oscillatory rather than growing
3. Accurately preserves the oscillatory nature and damping envelope
4. Computational cost (4 function evaluations per step) is justified by accuracy gain

The backward Euler method shows intermediate performance:

- Better than forward Euler due to implicit stability
- Maximum error of 0.33 rad is acceptable for some applications
- Requires iterative solution at each step

The forward Euler method, while simple, accumulates significant error:

- Maximum error exceeds 13 rad (nearly two oscillation cycles)
- Error grows over time, though remains bounded
- Unsuitable for precision applications

3.3.3 Physical Insights

The analytical solution reveals:

1. The system takes approximately $5\tau = 71.4$ s to settle to within 1% of equilibrium
2. The damping is so light ($\zeta = 0.01$) that approximately 150 oscillations occur during settling
3. The frequency is essentially unchanged from the undamped natural frequency: $\omega_d \approx \omega_n$
4. Initial energy is $E_0 = 0.5k\theta_0^2 = 2.56$ J, which dissipates according to $E(t) \approx E_0 e^{-2\zeta\omega_n t}$

CONCLUSIONS

This work successfully analyzed a mass-spring-damper system (pendulum variant) through both analytical and numerical methods, yielding several important findings.

Key Achievements:

1. **Equation of Motion Derivation**
   Using Lagrangian mechanics, we derived the governing equation:
   $$0.25\ddot{\theta} + 0.035\dot{\theta} + 11.2\theta = 0$$
   System characterization identified it as underdamped with damping ratio $\zeta = 0.010458$ and natural frequency $\omega_n = 6.6933$ rad/s.
2. **Analytical Solution**
   The closed-form solution for the underdamped case:
   $$\theta(t) = e^{-0.07t}(-0.6755\cos(6.6929t) - 0.007065\sin(6.6929t))$$
   describes exponentially decaying oscillations with period 0.939 s and time constant 14.29 s.
3. **Numerical Comparison**
   Three methods were implemented and compared:
   - Forward Euler: Max error 13.9 rad (unsuitable)
   - Backward Euler: Max error 0.33 rad (acceptable)
   - Runge-Kutta 4: Max error 3.98×10^{-6} rad (excellent)

   RK4 achieved five orders of magnitude better accuracy than forward Euler.

Theoretical Insights:

- Underdamped systems, unlike the unstable system in Task 1, do not exhibit exponential error amplification
- The oscillatory nature with damping makes the problem well-conditioned for numerical integration

– Even simple methods like forward Euler can remain stable, though accuracy suffers
– The analytical solution provides valuable physical insight into settling time, decay rate, and oscillation frequency

Practical Implications:
For vibration analysis of lightly damped mechanical systems:

1. Always prefer RK4 or higher-order methods for precision applications
2. The analytical solution is invaluable for parameter studies and design optimization
3. Phase portraits clearly visualize the approach to equilibrium
4. Energy analysis confirms physical consistency and identifies dissipation mechanisms

Comparison with Task 1:

– Task 1 (unstable ODE): Exponential growth, severe error amplification, RK4 essential
– Task 2 (damped oscillator): Bounded motion, manageable errors, RK4 still optimal but forward Euler usable for rough estimates
– Both tasks demonstrate that method selection must account for problem characteristics

Limitations and Extensions:
This study assumed small-angle approximations and linear damping. Future work could explore:

– Large-angle pendulum motion requiring numerical solution of the nonlinear equation
– Nonlinear damping models (quadratic drag)
– Forced vibrations with harmonic excitation
– Multi-degree-of-freedom systems
– Adaptive step-size methods for improved efficiency

Concluding Remarks:

The integration of analytical and numerical approaches provided comprehensive understanding of the damped pendulum system. The analytical solution served as an essential benchmark, revealing that for this well-behaved oscillatory problem, the Runge-Kutta 4 method delivers exceptional accuracy with reasonable computational cost. The work demonstrates that careful analysis of system characteristics—whether stable or unstable, oscillatory or monotonic—guides appropriate method selection for numerical simulation.

BIBLIOGRAPHY

[1] Ogata K. Modern Control Engineering. 5th ed. Prentice Hall, 2010.

[2] Thomson W.T., Dahleh M.D. Theory of Vibration with Applications. 6th ed. Springer, 2018.

[3] Rao S.S. Mechanical Vibrations. 6th ed. Pearson, 2017.

[4] Preumont A. Vibration Control of Active Structures: An Introduction // Solid Mechanics and Its Applications. 2018. Vol. 246.